Cost and Power-Consumption Analysis for Power Profile Monitoring in Optical Networks

Qiaolun Zhang[1,2], Patricia Layec[2], Annalisa Morea[3], Massimo Tornatore[1]

[1] Politecnico di Milano, Milan, qiaolun.zhang@mail.polimi.it,
[2] Nokia Bell Labs France, France, [3] Nokia, Vimercate, Italy

Abstract *We quantify and benchmark cost and power consumption of power profile monitoring (PPM) in opaque and transparent IPoWDM networks, comparing it to current optical time-domain reflectometer (OTDR) technology. Results show PPM is preferable even when PPM module adds 80% (50%) cost (power) to one transponder.*

Introduction

To achieve marginless operation in optical networks, massive monitoring is essential to collect comprehensive data on impairments in optical transmission and components. As deploying large amount of monitoring equipment results in elevated cost and power consumption, novel low-cost monitoring methods are being investigated[1]–[3]. A new technique, called *power profile monitoring (PPM)* is gaining increasing attention[1],[4],[5]. PPM monitors the entire lightpath (LP) by using only an additional post-processing monitoring component in the receiver, hence it does not require monitoring each amplifier along the optical line as in traditional monitoring with optical time-domain reflectometer (OTDR)[6]. Following the experimental demonstration of PPM capabilities[1],[2],[7], it becomes now important to quantify and compare the cost of PPM and OTDR on a network scale. This study aims to comprehensively quantify the cost and power consumption of PPM vs. OTDR for network monitoring. PPM technology is still evolving and its implementation (and hence its cost and power consumption) is not yet defined, e.g., it is still debated if PPM will come as a separate module or as submodule integrated in the receiver. Thus, in our analysis, we provide a sensitivity analysis for its cost and power consumption compared to a transponder to be used as a guideline for further implementation. Moreover, we observe that cost and power consumption are highly related to the network architectures, namely, *opaque* vs. *transparent* architectures, and we provide guidelines for a network-wide deployment of PPM that is more cost-effective and energy-efficient than OTDR.

Cost and Power Consumption Model

Fig. 1 shows how PPM modules can be deployed for both an opaque and a transparent IPoWDM network architectures as considered in our work[8]. Fig. 1(a) depicts the **opaque** case, where one monitoring module can be placed at each traversed node (except the source node) as opto-electronic conversion is performed at each intermediate node. The optical layer uses arrayed waveguide grating (AWG) for muxing and demuxing. Fig. 1(b) depicts the **transparent** case, where nodes are equipped with ROADMS to enable transparent optical bypass. This architecture allows end-to-end grooming and traffic regeneration at intermediate nodes with IP routers[8]. In this case, PPM modules can be deployed in each intermediate node with regeneration or at the destination node.

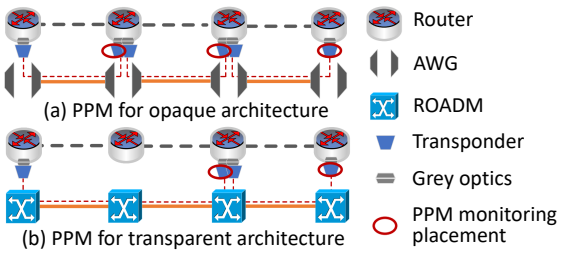

Fig. 1: Network-wide PPM deployment.

A possible network-wide OTDR deployment for transparent network architecture is shown in Fig. 2, which applies to also opaque architecture. Let us assume the network is denoted by $G = (N, E)$, where N is the set of physical nodes and E is the set of physical links. The number of spans in link (i, j) and the degrees of node i are denoted with $s_{(i,j)}$ and d_i, respectively. One OTDR card serves 4 fiber links. OTDRs are needed in every degree of nodes and every inline amplifier (one OTDR can cover both directions as in Fig. 2). Since we assume a bidirectional network with two fibers per degree, the number of OTDRs for node i is $\lceil 2d_i/4 \rceil$. The number of inline amplifiers that need to be monitored in link (i, j) is $max(0, s_{(i,j)} - 2)$ as the two spans close

to both end nodes are monitored with the OTDR for nodes. Hence, the number of OTDRs required in a network can be calculated using the equation below, which applies to both opaque and transparent architectures:

$$P = \sum_{(i,j)\in E} max(0, s_{(i,j)} - 2) + \sum_{i\in N} \lceil 2d_i/4 \rceil \quad (1)$$

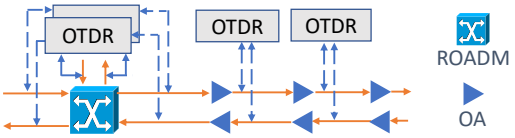

Fig. 2: Network-wide OTDR deployment.

Resource Allocation Problem

The problem of optimized monitoring placement (OMP) of PPM can be stated as: **Given** a network topology and a set of LPs, **decide** the placement of PPM modules, **constrained by** monitoring of all the links (*nb* a link is monitored if at least one LP traversing it is equipped with one PPM module), with the **objective** of minimizing the number of PPM modules. In this study, the initial set of LPs is obtained from an existing heuristic algorithm that minimizes the number of transponders used to serve requests[8].

We developed a new *OMP* algorithm to reduce the number of PPMs for monitoring. The *OMP* algorithm is designed leveraging existing effective heuristic algorithms for the set covering problem as in Ref.[9]. Note that this problem is different from the problem of choosing a set of ligthpath that allows performing fault localization on any link of the network (as in, e.g.,[10],[11]), that may involve selecting multiple LPs traversing the same link.

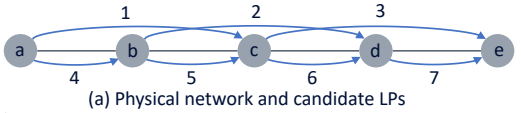

(a) Physical network and candidate LPs

Edge \ LP	1	2	3	4	5	6	7
(a,b)	1	0	0	1	0	0	0
(b,c)	1	1	0	0	1	0	0
(c,d)	0	1	1	0	0	1	0
(e,e)	0	0	1	0	0	0	1
Sum	2	2	2	1	1	1	1

Stage1: obtain paths covering maximum number of edges (path 1,2,3)

Stage2: select the path that affects the minimum number of other paths (path 1)

(b) Selection of path for monitoring placement

Fig. 3: Illustration of the *OMP* algorithm.

The *OMP* algorithm is illustrated in Fig. 3, where we consider only one direction, for sake of simplicity. Fig. 3(a) shows a simple physical linear network and seven candidate LPs. No LP is longer than two hops, e.g., due to the limited reach of transponders. Starting from an empty list of LPs, *OMP* iteratively adds a new LP to the list, by choosing greedily the LP that can monitor more links until all the links are monitored as shown in Fig. 3(b). An element of the table in Fig. 3 is equal to one when the LP, corresponding to the column of that element, contains the corresponding edge. At each iteration, the algorithm requires two stages. In stage 1, the algorithm identifies the LPs that allow to cover (monitor) the maximum number of edges, i.e., it selects the columns with the maximum sum of its elements (listed in the last row of the table in Fig. 3(b)). In stage 2, the algorithm selects, among the columns identified in stage 1, the column (i.e., the LP) that affects the minimum number of other LPs (an edge of another LP is affected if both LPs have an element equal to 1 in the same row). In case of ties, *OMP* randomly selects a column. In Fig. 3 (b), after selecting LPs 1, 2, 3 in phase 1, stage 2 selects LP 1. The affected edges of the other LPs are marked with red rows and red font in Fig. 3. We identify that LP 1 may affect LPs 2, 4, and 5. As all edges in LPs 4 and 5 are already monitored and therefore will not be selected, only one LP is considered affected. In the current iteration, the algorithm can select LP 1, which only affects one LP. In the next iteration, the algorithm will select LP 3, and all the edges will be monitored. In summary, *OMP* reduces the PPM modules from 9 (one for each LP) to 2.

Case Studies and Results

We perform our numerical evaluations on both a national-scale and a continental-scale topology, the 14-node Japan (J14)[12] and the 14-node NSF (N14), respectively[13]. Each fiber operates on a 6-THz C-band. We consider two architectures, i.e., opaque (the cases w/o *OMP* are named as *Op-O* and *Op*, respectively) and transparent (the cases w/o *OMP* are named as *Tr-O*, *Tr*, respectively) architectures, which are compared to the OTDR deployment. The requested data rate is randomly generated from 100 Gb/s to 400 Gb/s. We increase the number of requests until 1% of requests are blocked in transparent architecture, and we use the corresponding carried traffic for both opaque and transparent architectures. The normalized cost (energy) of a transponder and of an OTDR module is 4 (8) and 0.2 (0.25), respectively. We vary the cost and power consumption of a PPM module compared to that of a transponder. All the results are averaged out of 10 instances.

Number of modules. Let us first compare the number of monitoring components (i.e., either PPM or OTDR modules) used in J14 and N14

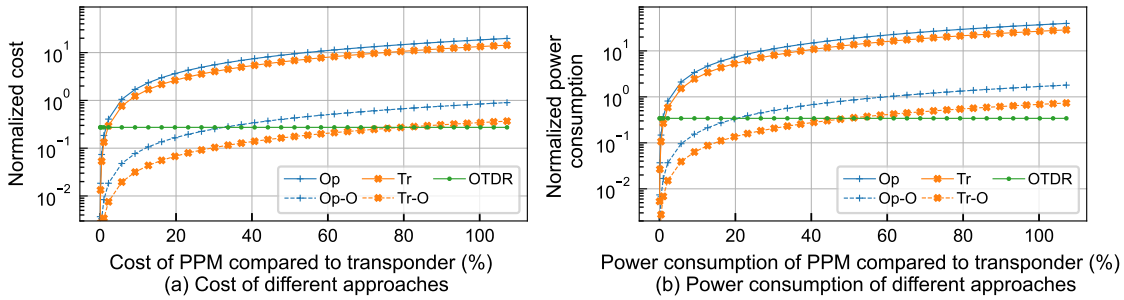

Fig. 4: Cost of and power consumption of different approaches in NSF topology

topologies, as reported in Tab. 1. First, without *OMP*, the number of PPM modules for *Op* is 22 times that of OTDR in J14, which is reduced to 3.4 times in N14 because the OTDR shows an 600% increase in N14 compared to J14, owing to the increased number of spans. With *OMP*, the number of PPM modules for *Op-O* is reduced to the number of edges in the network as one edge is monitored with one PPM module. Note that in N14 for *Op-O*, the number of PPM modules even decreased to only 15% of OTDRs. Moreover, transparent architectures can further reduce up to 64% PPM modules by bypassing nodes. Instead, the number of OTDRs only depends on network topology rather than network architectures.

Tab. 1: Number of monitoring components on J14 and N14

Scenarios	Op	Tr	Op-O	Tr-O	OTDR
J14	855	552	44	16	39
N14	924	750	42	17	273

Normalized cost in N14. Fig. 4(a) illustrates the normalized cost of monitoring per Tb/s for N14. We define the x-axis value of the point where PPM's cost/power consumption is equal to OTDR as *crossing value*, which is also reported in Tab. 2. The cases with *OMP* have much smaller crossing values than the cases without *OMP*, showing that *OMP* is fundamental to lower PPM monitoring costs. Without *OMP*, the cost of one PPM must be less than 1.5% and 2.0% of one transponder for *Op* and *Tr*, respectively to compete with OTDR. However, with *OMP*, the cost of PPM should be below 33% and 80% of the cost of transponder for *Op-O* and *Tr-O*, respectively, to compete with OTDR. Note that the cost difference between *Op-O* and *Tr-O* is due to bypassing of nodes in the transparent architecture.

Normalized power consumption in N14. Fig. 4(b) plots the power consumption of PPM compared to OTDR. To consume less power than OTDR, PPM needs to have lower complexity. Without *OMP*, the power consumption of PPM relative to one transponder must be less than 0.9% and 1.3% of the transponder's power consumption. With *OMP*, the power consumption of PPM can be up to 20% and 50% of the transponder's power consumption for opaque and transparent architectures, respectively.

Tab. 2: crossing values of PPM with OTDR in N14(J14).

Scenarios	Op	Tr	Op-O	Tr-O
Cost	1.5(0.2)	2.0(0.4)	33(4)	80(12)
Power consumption	0.9(0.1)	1.3(0.2)	20(3)	50(8)

Normalized cost and power consumption in J14. The overall trends of cost and power consumption in J14 are similar to N14. Tab. 2 reports the crossing values for J14 in brackets. Different from N14, PPM can perform better than OTDR only with a much lower cost and power consumption than one transponder. This is because less OTDRs are deployed in links in a smaller topology Specifically, PPM's cost and power consumption are reduced to approximately 0.2% and 0.1% for *Op*, and 0.4% and 0.2% for *Tr*, respectively. Moreover, with *OMP*, the cost and power consumption are reduced from 80% to 12% and 50% to 8% for transparent architecture.

Conclusion

Following the recent experimentation of PPM as novel monitoring solution, in this work we investigated the problem of optimized monitoring placement for PPM, and we quantified the cost and power consumption of PPM compared to OTDR to provide guidelines for deployment of PPM modules. Results show that, for a nation-wide topology as J14, cost/power consumption of the PPM should be below 12% (8%) of that of a transponder to compete with OTDR. Instead, in a larger continental-wide topology as N14, PPM's cost/power consumption should be below 80% (50%) of that of a transponder. This means that cost and power consumption of PPM are not limiting factors for PPM deployments, as PPM is not expected to have such a high cost and power consumption.

This work was supported by the Italian Ministry of University and Research (MUR) and the European Union (EU) under the PON/REACT project and partly funded by EU Horizon 2020 B5G-OPEN Project (grant agreement 101016).

References

[1] A. May, F. Boitier, A. C. Meseguer, *et al.*, “Longitudinal power monitoring over a deployed 10,000-km link for submarine systems”, in *Optical Fiber Communication Conference (OFC)*, 2023, Tu2G.3.

[2] T. Sasai, E. Yamazaki, M. Nakamura, and Y. Kisaka, “Closed-form expressions for fiber-nonlinearity-based longitudinal power profile estimation methods”, in *European Conference on Optical Communication (ECOC)*, 2022, Tu1D.6.

[3] C. Hahn, J. Chang, and Z. Jiang, “Monitoring of generalized optical signal-to-noise ratio using in-band spectral correlation method”, in *European Conference on Optical Communication (ECOC)*, 2022, Tu5.38.

[4] T. Tanimura, S. Yoshida, K. Tajima, S. Oda, and T. Hoshida, “Fiber-longitudinal anomaly position identification over multi-span transmission link out of receiver-end signals”, *IEEE/OSA Journal of Lightwave Technology*, vol. 38, no. 9, pp. 2726–2733, 2020.

[5] A. May, F. Boitier, E. Awwad, P. Ramantanis, M. Lonardi, and P. Ciblat, “Receiver-based experimental estimation of power losses in optical networks”, *IEEE Photonics Technology Letters*, vol. 33, no. 22, pp. 1238–1241, 2021.

[6] Y. R. Zhou, K. Smith, P. Weir, *et al.*, “Field trial demonstration of novel optical superchannel capacity protection for 400g using dp–16qam and dp–qpsk with in-service otdr fault localization”, in *Optical Fiber Communication Conference (OFC)*, 2016, W3B.3.

[7] I. Kim, O. Vassilieva, R. Shinzaki, M. Eto, S. Oda, and P. Palacharla, “Robust longitudinal power profile estimation in optical networks using mmse with complex scaling factor”, in *Optical Fiber Communication Conference (OFC)*, 2023, W4H.6.

[8] Q. Zhang, A. Morea, and M. Tornatore, “A pragmatic power-consumption analysis for ipowdm networks with zr/zr+ modules”, in *European Conference on Optical Communication (ECOC)*, 2022, We5.64.

[9] F. J. Vasko, Y. Lu, and K. Zyma, “What is the best greedy-like heuristic for the weighted set covering problem?”, *Operations Research Letters*, vol. 44, no. 3, pp. 366–369, 2016.

[10] C. Delezoide, P. Ramantanis, L. Gifre, F. Boitier, and P. Layec, “Field trial of failure localization in a backbone optical network”, in *European Conference on Optical Communication (ECOC)*, 2021, pp. 1–4.

[11] K. Christodoulopoulos, N. Sambo, and E. Varvarigos, “Exploiting network kriging for fault localization”, in *Optical fiber communication conference (OFC)*, 2016, W1B–5.

[12] M. Ibrahimi, H. Abdollahi, C. Rottondi, *et al.*, “Machine learning regression for QoT estimation of unestablished lightpaths”, *IEEE/OSA Journal of Optical Communications and Networking*, vol. 13, no. 4, B92–B101, Apr. 2021.

[13] B. G. Bathula and J. M. Elmirghani, “Constraint-based anycasting over optical burst switched networks”, *IEEE/OSA Journal of Optical Communications and Networking*, vol. 1, no. 2, A35–A43, 2009.